

# Malformations of Cortical Development: From Postnatal to Fetal Imaging

Tally Lerman-Sagie, Zvi Leibovitz

**ABSTRACT:** Abnormal fetal corticogenesis results in malformations of cortical development (MCD). Abnormal cell proliferation leads to microcephaly or megalencephaly, incomplete neuronal migration results in heterotopia and lissencephaly, neuronal overmigration manifests as cobblestone malformations, and anomalous postmigrational cortical organization is responsible for polymicrogyria and focal cortical dysplasias. MCD comprises various congenital brain disorders, caused by different genetic, infectious, or vascular etiologies and is associated with significant neurological morbidity. Although MCD are rarely diagnosed prenatally, both dedicated multiplanar neurosonography and magnetic resonance imaging enable good demonstration of fetal cortical development. The imaging signs of fetal MCD are: delayed or absent cerebral sulcation; premature abnormal sulci; thin and irregular hemispheric parenchyma; wide abnormal overdeveloped gyri; wide opening of isolated sulci; nodular bulging into the lateral ventricles; cortical clefts; intraparenchymal echogenic nodules; and cortical thickening. The postnatal and prenatal imaging features of four main malformations of cortical development—lissencephaly, cobblestone malformations, periventricular nodular heterotopia, and polymicrogyria—are described.

**RÉSUMÉ:** Malformations du développement cortical : de l'imagerie postnatale à l'imagerie fœtale. Au stade fœtal, un processus anormal de corticogénèse peut s'expliquer par des malformations du développement cortical (MDC). Une prolifération anormale des cellules entraîne alors des cas de microcéphalie ou de macrocéphalie ; une migration neuronale incomplète, des cas d'hétérotopie et de lissencéphalie ; une migration neuronale excessive, des malformations de type pavimentaire ; enfin, une anomalie post-migratoire de l'organisation corticale, des cas de polymicrogyrie et de dysplasie corticale focale. Les MDC incluent plusieurs anomalies congénitales du cerveau causées par différentes étiologies génétiques, infectieuses ou vasculaires ; elles sont aussi associées à une morbidité neurologique notable. Bien que les MDC soient rarement diagnostiquées au stade prénatal, tant la reconstruction multiplanaire (RMP) (multiplanar neurosonography) que l'imagerie par résonance magnétique (IRM) permettent de bien observer le développement cortical fœtal. Parmi les signes de MDC fœtal, mentionnons les suivants : une sulcation cérébrale absente ou retardée ; des sillons (sulci) anormaux chez le prématuré ; un tissu parenchymateux mince et irrégulier ; des circonvolutions cérébrales (gyri) dont la largeur est anormalement disproportionnée ; l'ouverture d'un sillon (sulci) isolé ; une voussure des nodules dans les ventricules latéraux ; des fissures dans la région corticale ; des nodules du tissu intra-parenchymateux dépistés par échographie ; et un épaississement de la région corticale. Les caractéristiques de quatre principales MDC (lissencéphalie, de type pavimentaire, hétérotopie nodulaire péri-ventriculaire et polymicrogyrie) en termes d'imagerie prénatale et postnatale sont décrites dans le présent article.

**Keywords:** Magnetic resonance imaging, Ultrasound, Malformations of cortical development, Lissencephaly, Cobblestone malformation, Periventricular nodular heterotopia, Polymicrogyria

doi:10.1017/cjn.2016.271

Can J Neurol Sci. 2016; 43: 611-618

## INTRODUCTION

Malformations of cortical development (MCD) comprise myriad disorders related to disruption of the complex process of cortex formation, caused by various genetic, infectious, or vascular etiologies. MCD are associated with significant neurological morbidity, including intellectual disability, epilepsy, and motor dysfunction.<sup>1</sup>

The discovery of chromosome 17p13.3 deletions, followed by mutations in LIS1, in children with lissencephaly in 1983, marked the beginning of a new era of understanding the genetic basis and the pathogenesis of brain malformations.<sup>2</sup>

Since then, the accelerated rate of gene discovery, particularly with the introduction of next-generation sequencing (NGS), has uncovered a large number of novel genes associated with malformations of cortical development.<sup>3</sup>

Although early embryonic malformations of dorsal and ventral induction (including cephalic neural tube defects and holoprosencephaly) are frequently associated with an anomalous cerebral cortex, the MCD are related to later events in fetal corticogenesis that are controlled by three overlapping developmental stages:

neural stem cell proliferation, migration, and organization. Abnormal cell proliferation may cause primary microcephaly, megalencephaly, or hemimegalencephaly. Failure of initial neuronal migration results in periventricular heterotopia. Disorders of later migration cause disruption of the normal six-layered cortex (classical lissencephaly) and subcortical band heterotopia; however, neurons that fail to stop at their intended cortical destination and continue to migrate onto the cortical surface result in cobblestone malformation. Finally, abnormal postmigrational development underlies polymicrogyria (PMG) and focal cortical dysplasias. Because of the overlap between the developmental stages, disorders of corticogenesis may present with complex cortical malformations.<sup>4</sup>

From the Fetal Neurology Clinic (TL-S, ZL); Pediatric Neurology Unit (TL-S, ZL), Wolfson Medical Center, Holon, Israel; Sackler Faculty of Medicine, Tel-Aviv University, Tel-Aviv, Israel (TL-S); Ultrasound Unit, Department of Obstetrics and Gynecology, Bnai Zion Medical Center, Haifa, Israel (ZL).

RECEIVED DECEMBER 20, 2015. FINAL REVISIONS SUBMITTED APRIL 9, 2016. DATE OF ACCEPTANCE APRIL 19, 2016.

Correspondence to: Tally Lerman-Sagie, Pediatric Neurology Unit, Wolfson Medical Center, Holon, Israel. Email: asagie@post.tau.ac.il

The diagnosis of MCD requires high-resolution multiplanar magnetic resonance imaging because of its ability to demonstrate excellent contrast resolution between white matter and gray matter, to characterize topographically the development of cortical gyri and sulci, and to analyze accurately the formation of white matter and stages of myelination.<sup>5</sup>

MCD are rarely diagnosed prenatally. This can be explained by the late gestational appearance of their typical morphological features, usually beyond the recommended time of the routine fetal anatomical sonographic scan (19-23 weeks). Moreover, the low antenatal MCD detection rate may be related to the common standards of basic fetal brain ultrasound imaging, restricted to the axial planes at the level of the lateral ventricles, thalami, third ventricle, cavum septi pellucidi, cerebellum, and cisterna magna.<sup>6</sup> Performance of ultrasonography only in the axial plane may lead to misdiagnosis of MCD that are evident only in the coronal and sagittal planes; however, both dedicated neurosonography and fetal magnetic resonance imaging (MRI) are able to accurately depict fetal cortical malformations, and many articles have been published in the past decade describing these achievements.

Sonography is the most important imaging method for prenatal malformation screening because it is noninvasive, widely available, and safe for both mother and fetus. The ultrasonographic approach to evaluating the fetal brain is based on the classic transabdominal visualization of three different axial planes: the transventricular, the transthalamic, and the transcerebellar (not sufficient for optimal depiction of malformations of the cortex and midline brain structures), supplemented by a more comprehensive, multiplanar approach, in which coronal and sagittal planes are added to the axial ones by a transvaginal or transabdominal scan.<sup>7</sup>

MRI was introduced into fetal imaging more than 30 years ago and is a valuable complementary tool in the imaging of structural anomalies of the fetal brain.

Implementation of fast and ultrafast sequences has allowed reduction of acquisition time, which has subsequently decreased artifacts resulting from fetal movements. Fetal MRI has higher contrast resolution than prenatal sonography and enables better differentiation of normal from abnormal tissue.<sup>8,9</sup>

Fetal MRI is performed primarily using ultrafast MRI techniques known as single-shot, fast spin-echo or half-Fourier acquired single-shot turbo spin-echo. Using these rapid-pulse sequences, a single T2-weighted image can be acquired in less than 1 second, reducing the likelihood of fetal motion during image

acquisition.<sup>7,8</sup> When the fetal brain is being evaluated, images are obtained with a section thickness of 3 mm with no gap, in axial, sagittal, and coronal planes.<sup>8-11</sup>

With the recent application of advanced MRI techniques, an opportunity to investigate the developing brain is available beyond the qualitative morphologic evaluation.<sup>12,13</sup>

The earliest recognition of MCD is reported at the 22nd week of gestation in fetuses with Miller-Dicker and Walker-Warburg syndrome by demonstration of abnormal formation of the Sylvian fissures,<sup>14</sup> which is enabled by the knowledge of their normal imaging pattern of development (Figure 1A-C).<sup>15-18</sup>

Delayed or absent cerebral sulcation is considered a principal feature of fetal MCD. Several additional indicative sonographic signs have been described: premature abnormal sulci; thin and irregular cortical mantle; wide abnormal overdeveloped gyri; wide opening of isolated sulci; nodular bulging into the lateral ventricles; cortical clefts; and intraparenchymal echogenic nodules.<sup>6,7,19</sup>

In late gestational weeks, the diagnosis of MCD by MRI is more accurate than by ultrasound, primarily because of brain sonographic shadowing caused by the skull bones and technical difficulties in attaining an appropriate acoustic window. MRI can add information and clarify the different gyration patterns that can be difficult to discern by ultrasound.<sup>20</sup>

The MRI signs suggestive of MCD are similar to ultrasound and include: delayed cortical development; dysgenesis of the Sylvian fissure; delayed sulcal appearance; cortical thickening; irregularity of the ventricular wall; absence or abnormal appearance of fissures; abnormal, asymmetric gyri; and discontinuous cortex.<sup>14,21</sup>

Because MCD were initially depicted in children, in this article, we first describe the postnatal imaging features, and then the etiology (genetic or disruptive) followed by the fetal sonographic and MRI findings. We demonstrate four main malformations of cortical development: lissencephaly, cobblestone malformations, periventricular nodular heterotopia, and PMG.

#### LISSENCEPHALY TYPE I

Lissencephaly is defined as a smooth brain and characterized by abnormalities in the width of the gyri and the thickness of the cortex. The neocortex of lissencephalic patients lacks normal cortical lamination and contains two to four layers instead of six.<sup>22</sup> Classic or type 1 lissencephaly appears as complete or incomplete agyria.



**Figure 1:** Normal and abnormal development of the operculum at 23 gestational weeks (transabdominal ultrasound in the axial plane). (A) Normal; note the square-shaped operculum. (B) Lissencephaly; note the minimal opercular indentation. (C) Generalized PMG; note the shallow irregular opercular shape.

The degree of agyria is graded. The complete form is characterized by a smooth surface of the entire brain. In the incomplete form, which is the more commonly seen type, there is a gradient of severity either anterior to posterior or posterior to anterior depending on the genetic defect.

The important postnatal MRI findings of classical lissencephaly are: a hourglass configuration of the brain with large ventricles in the complete form; a thick, smooth thickened cortex

(>10 mm) separated from a deep layer of neurons by a “cell sparse layer”; thin subcortical white matter; lack of gray-white matter interdigitations; and shallow Sylvian fissures (Figure 2E,F).<sup>1,23</sup> Lissencephaly is usually symmetric. Agenesis of the corpus callosum or cerebellar hypoplasia can be associated findings depending on the affected gene. The known genes are: *LIS1*, *ARX*, *RELN*, *VLDLR*, *ACTB*, *ACTG1*, *DCX*, *DYNC1H1*, *KIF2A*, *TUBA1A*, *TUBB2B*, and *TUBG1*.<sup>22</sup>

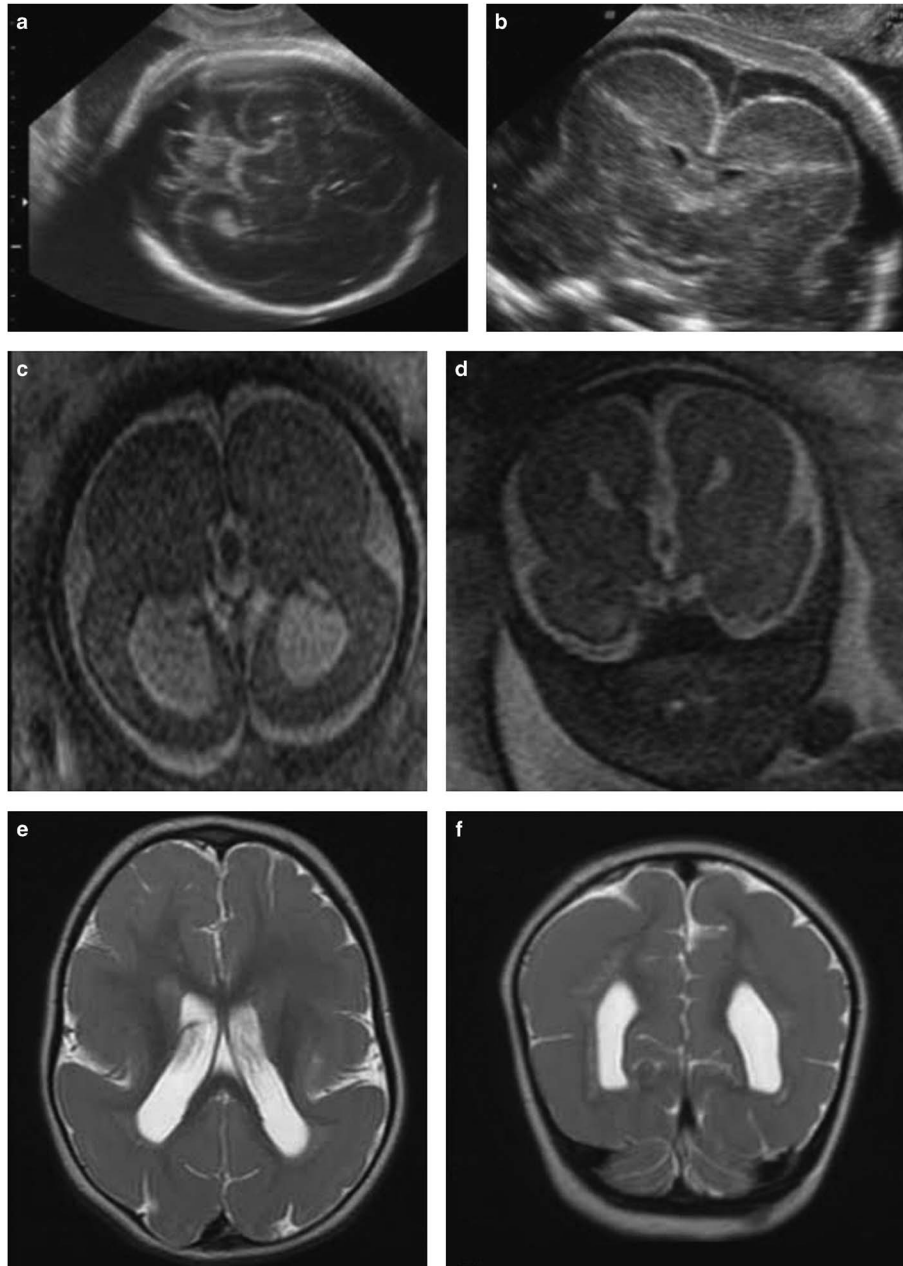


**Figure 2:** Lissencephaly type I, prenatal and postnatal imaging (three different cases). (A, B) Ultrasound images (axial and coronal) at 23.5 weeks' gestation. Note the nearly complete absence of the Sylvian fissures. (C, D) MRI (axial and coronal) at 33 weeks' gestation. Note thick featureless cortex, “figure of eight” brain configuration, and agenesis of the corpus callosum. (E, F) MRI (axial and coronal) at 1 year of age. Note wide gyri with thick cortex, decreased interdigitation of the white matter, and a posterior-to-anterior gradient (patient with a *LIS1* mutation).

### Prenatal Diagnosis

Lissencephaly type 1 and Miller-Dieker syndrome are usually diagnosed in utero after 27 to 30 weeks' gestation, either by detailed neurosonography or MRI, by demonstrated lack of development of the primary sulci that should already be present.

Mild ventriculomegaly and delayed opercular development are the earliest signs and can be depicted by 23 weeks of gestation in fetuses at risk.<sup>6</sup> Lissencephaly is diagnosed by demonstration of dysgenesis of the Sylvian fissure, delayed sulcal appearance, callosal abnormality, and cortical thickening (Figure 2A-D).<sup>24,25</sup> Sometimes, zones of normal cortex and zones of pachygyric or

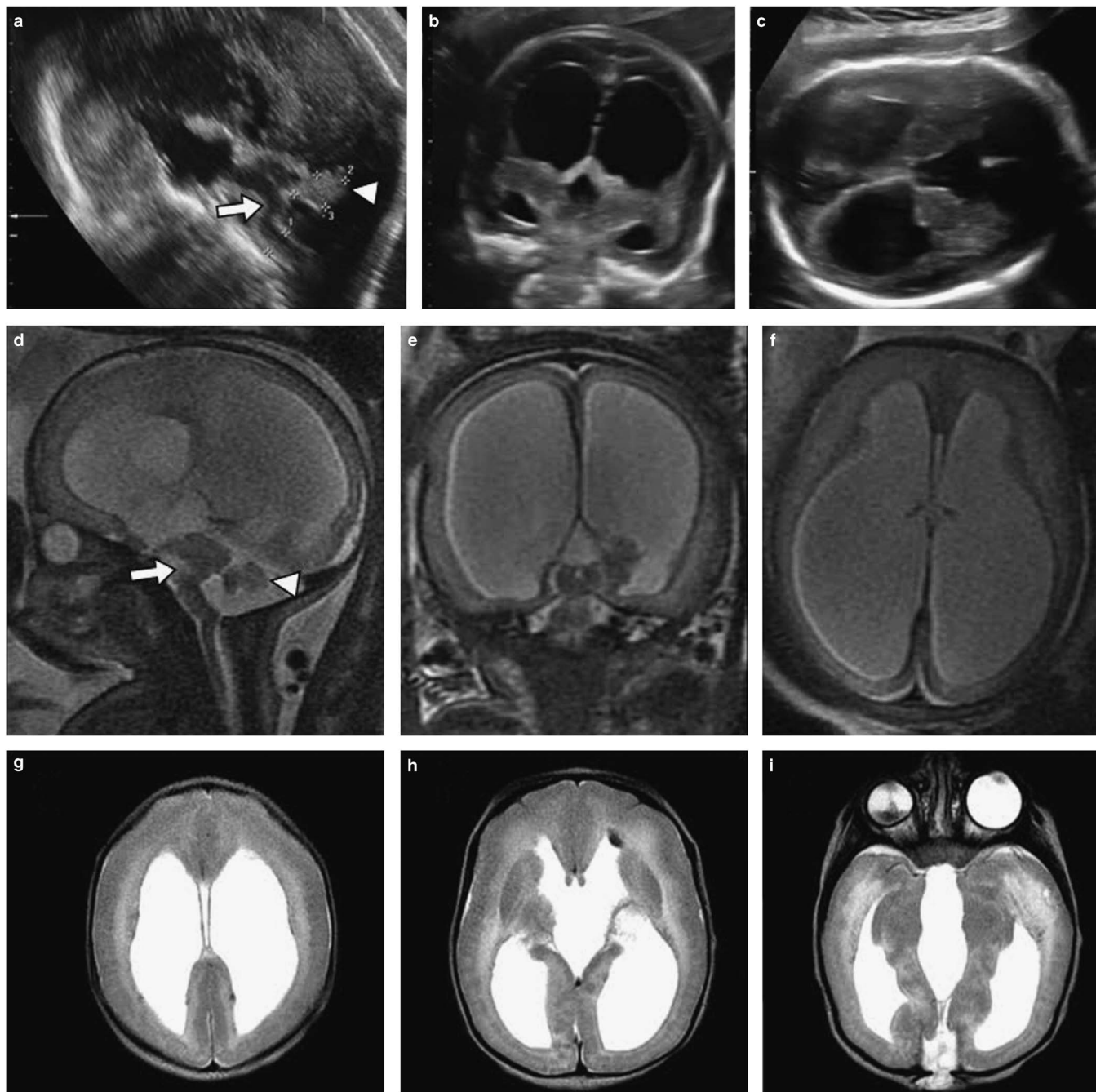


**Figure 3:** Cobblestone malformation, prenatal and postnatal imaging (three different cases). (A-C) Ultrasound images at 26 gestational weeks (sagittal, coronal, and axial). Note severe ventriculomegaly, absence of the Sylvian fissures, no primary sulcation, “Z”-shaped (kinked) brainstem (arrow), and hypoplastic vermis (arrowhead). (D-F) Fetal MRI, sagittal, coronal, and axial images at 34 weeks demonstrate “Z”-shaped (kinked) brainstem (arrow), hypoplastic vermis (arrowhead), severe ventricular dilatation, and abnormal sulcation with thin cortex (courtesy of Dr. Chen Hoffman). (G-I) Neonatal MRI, sequential axial images. Note triventricular hydrocephalus, thick irregular cortex with a cobblestone appearance, increased T2 signal from white matter with no interdigitation, retinal detachment, phthisis bulbi of the right eye, and posterior encephalocele. (In addition, small intraventricular blood clots in G and H).

agyric cortex alternate. The abnormal opercular formation is responsible for a “figure-eight” shaped brain.<sup>14</sup> Sometimes, the genetic defect can be suspected based on the gradient of the anomaly (anterior > posterior-*DCX* or posterior > anterior-*LIS1*), the fetal gender (male-*DCX*, *ARX*), associated brain anomalies (agenesis of corpus callosum-*ARX*, cerebellar hypoplasia-*RELN*, and abnormal basal ganglia-*TUBA1A*).

### COBBLESTONE MALFORMATION

Cobblestone malformation, formerly called type 2 lissencephaly, is characterized by a nodular cortical surface accompanied by ocular anomalies and congenital muscular disorders.<sup>23</sup> Cobblestone malformations have been divided into three different groups based on severity, with Walker-Warburg syndrome being the most severe form, Fukuyama congenital muscular dystrophy the mildest form, and muscle-eye brain disease being the moderate form. Congenital muscular dystrophy is a key feature.

The structural abnormalities result from lack of connection of the radial glia to the pial limiting membrane and neuronal overmigration through pial gaps.<sup>4</sup>

There are many different MRI appearances: posterior pachygyria/ agyria, anterior PMG-like appearance, cerebellar dysplasia/cysts, and delayed/absent myelination in central regions. It is associated with fused colliculi, a small pons, a dysmorphic mesencephalon, a dorsal pontomedullary kink, vermian hypogenesis, and cerebellar hypoplasia. Microphthalmia and retinal dysplasia (small and dysplastic globe) are commonly seen as are hydrocephalus and posterior cephalocele.<sup>5,22,23</sup> Some have associated anomalies of the corpus callosum and septum pellucidum (Figure 3G-I).

The currently known genes are: *FKTN*, *POMT1*, *POMT2*, *POMGnT1*, *FKRP*, *LARGE*, and *GPR56*.<sup>3</sup>

### Prenatal Diagnosis

The prenatal diagnosis of Walker-Warburg syndrome has been reported in families at risk.<sup>26,27</sup> An early diagnosis in the first trimester may be made if there is a cephalocele.<sup>26</sup> Other suggestive findings are early enlargement of the lateral ventricles, abnormal vermis, retinal detachment,<sup>28</sup> cataract, abnormal sulcation,<sup>29</sup> kinked brainstem, and bifid pons (Figure 3A-F).<sup>29-32</sup>

### PERIVENTRICULAR NODULAR HETEROTOPIA

Heterotopia occurs when neurons originating in the periventricular region fail to migrate, leaving tracks or nodules of normal neurons in abnormal locations adjacent to the ependymal lining or in subcortical topography.<sup>5</sup> Based on MRI scans, there are three types of heterotopia: periventricular nodular heterotopia, focal subcortical heterotopia, and band heterotopia. Patients usually present with seizures and developmental delay.

Periventricular (subependymal nodular) heterotopias (PNH) are often bilateral and placed adjacent to the walls of the lateral ventricles, frequently in the peritrigonal regions, the temporal and occipital horns.<sup>23</sup> The characteristic appearance of nodular heterotopia is small, round- or oval-shaped nodules, isointense with gray matter, located in the subependymal layer and projecting into the ventricular lumen (Figure 4C).

PNH can be unilateral, bilateral, symmetric, asymmetric, anterior, central, posterior, inferior, “string of pearls,” contiguous, multinodular, laminar, or “ribbon like.” Posterior PNH have a significantly higher incidence of associated hippocampal, cerebellar, and brain stem anomalies compared with anterior or diffuse PNH. Diffuse PNH have associated agenesis of the corpus callosum and mega cisterna magna.<sup>23</sup>

Injury to, or denudation of, the neuroependyma is an important factor in the formation of periventricular nodular heterotopia, rather than a cell-intrinsic motility defect.<sup>4</sup>

Genetic etiology is not assigned in most cases. Two loci have been identified: X-linked PNH results from mutations in the filamin A gene (*FLNA*), and a rare autosomal recessive disorder of PNH with microcephaly results from mutations in *ARFGEF2*. The majority of familial cases are the result of an alteration in *FLNA*, in contrast to sporadic PNH cases, in which only 20% to 24% have been identified with a mutation in this gene. PNH can be associated with microdeletion syndromes.<sup>33</sup>

### Prenatal Diagnosis

PNH should be considered in utero when ultrasound depicts an irregular lateral ventricular wall with indentations of periventricular tissue (Figure 4A). The sonographic diagnosis is difficult, particularly when the lateral ventricle width is normal.

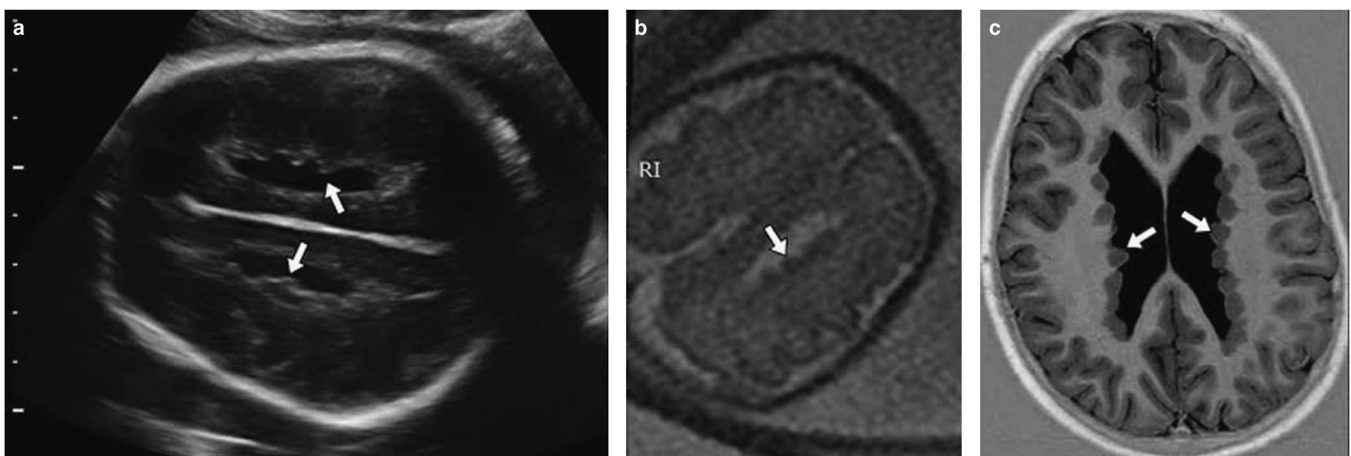


**Figure 4:** Periventricular nodular heterotopia, prenatal and postnatal imaging. (A) Ultrasound axial image at 32 gestational weeks. (B) MRI of the same fetus at 33 weeks. Note nodular bulging into the ventricles (arrows). (C) Adult MRI (axial image) showing classical periventricular nodular heterotopia (arrows) with a “string of pearls” appearance.

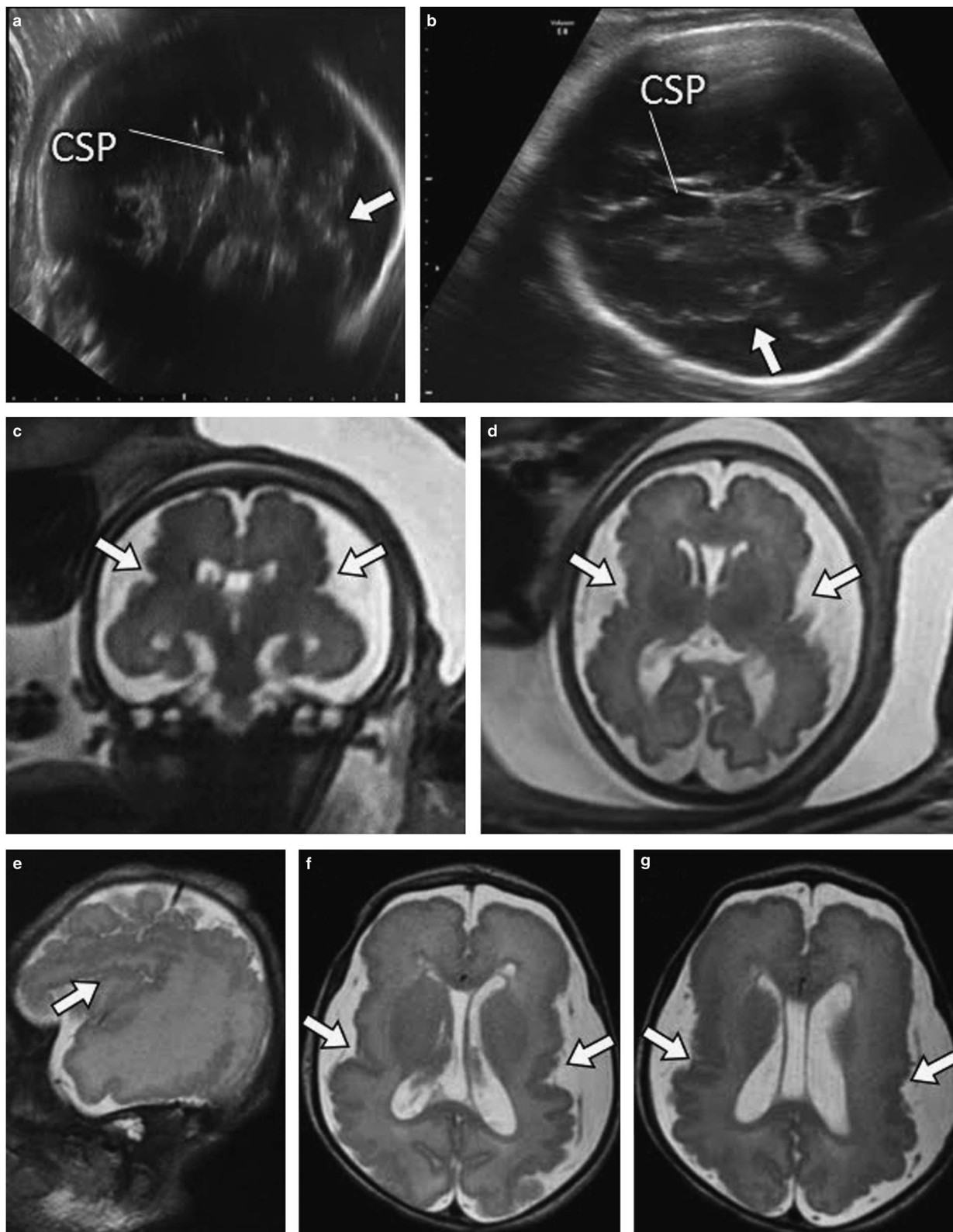


**Figure 5:** Generalized polymicrogyria in patients with DiGeorge syndrome. (A, B) Ultrasound images (coronal and axial) at 32 weeks' gestation. Note open, dysmorphic operculum with irregular cortical surface (arrows) facing enlarged perisylvian subarachnoid space. CSP, cavum septi pellucidum. (C, D) MRI scans of the same fetus (coronal and axial) at 33 weeks' gestation. Note diffuse bilateral polymicrogyria, open dysmorphic opercula (arrows), and lean brain parenchyma with abundant cerebrospinal (CSF) spaces around the hemispheres. (E-G) Neonatal MRI images (E, parasagittal; F-G, axial). Note generalized polymicrogyria, open dysmorphic opercula (arrows), and expanded periopercular CSF spaces.

MRI demonstrates multiple small nodular subependymal foci of low signal intensity, isointense to the germinal matrix, similar to that of the gray matter, located in the margins of the lateral ventricles (Figure 4B). They cannot be distinguished reliably from the subependymal nodules seen in tuberous sclerosis; therefore, it is important to search for other manifestations of tuberous sclerosis, such as cortical hamartomas and cardiac rhabdomyomas. A mega cisterna magna, which can be seen in females with filamin A mutations, may be the initial abnormality and, in association with diffuse periventricular nodules with a string of pearls appearance, may suggest the prenatal diagnosis of *FLNA* mutations.<sup>34-36</sup> In these cases, it is mandatory to obtain a maternal MRI scan that can demonstrate similar findings. Heterotopia may not be recognized when the nodules are single or small.

### POLYMICROGYRIA

Bielschowsky first used the term “polymicrogyria” in 1916 to describe a cerebral or cerebellar cortex with multiple excessive small convolutions. PMG is caused by an interruption in normal cerebral cortical development in the late neuronal migration or early post-migrational development periods.<sup>4</sup> It is not a single entity, but a spectrum of cortical malformations with the common feature being excessive gyration.<sup>37</sup> All have in common a derangement of the normal six-layered lamination of the cortex, an associated derangement of sulcation, and fusion of the molecular layer across sulci.<sup>38</sup>

The wide spectrum of PMG disorders has different causes, gross appearance, association with various accompanying malformations or disruptions, and microscopic appearance, making it difficult to understand and properly classify. It has been classified mainly according to imaging patterns.<sup>38,39</sup> There is overlap between true PMG and other disorders with a similar imaging appearance such as the cobblestone malformations.

PMG affects variable portions of the cerebral cortex: it may be focal, multifocal, or diffuse; it may be unilateral, bilateral, and asymmetrical; or bilateral and symmetrical. The most common location (in 60% to 70% of cases) is around the Sylvian fissure, particularly the posterior aspect of the fissure; however, any part of the cerebral cortex, including the frontal, occipital, and temporal lobes, can be affected. PMG may be an isolated malformation or it may be associated with other brain malformations.<sup>38</sup>

MRI shows excessive cortical gyration with an aspect of cortical thickening and shallow sulci and irregularity of the gray-white matter interface. In cases of the perisylvian syndrome, there is PMG surrounding the operculum with enlarged and vertically oriented Sylvian fissures, extending to the parietal lobes (Figure 5E-G).<sup>5</sup>

The etiology of PMG includes: congenital infection (particularly cytomegalovirus infection, localized or diffuse in utero ischemia, or genetic disorders). The known genes include: *SRPX2*, *TBR2*, *ARFGEF2*, *NDE1*, *WDR62*, *PAX6*, *KIAA1279*, *RAB3GAP1*, *RAB3GAP2*, *TUBA1A*, *TUBB2B*, *TUB3*, *TUBA8*, *TUBB5*, *FOXP2*, and *RTTN*.<sup>3</sup>

### Prenatal Diagnosis

The cortical changes of PMG take place late in pregnancy and appear as localized and/or generalized absence of normal sulcation with multiple abnormal infoldings of the affected cortex.<sup>8</sup> In young fetuses (younger than 24 weeks), the identification of this cortical malformation is quite difficult and the

manifestations on both ultrasound and MRI are subtle. They include presence of sulci that are not expected according to the gestational age; abnormal opercular development (Figure 1C); an irregular surface of the brain; and absence of the normal signal of the cortical ribbon. Late in pregnancy, the MRI features are similar to what is known in the postnatal period: packed and serrated microgyri, irregular gray-white matter junction, and an aberrant and asymmetrical sulcal pattern.<sup>40</sup> The most frequent MRI presentation diagnosed in utero demonstrates mild ventricular dilatation associated with numerous sulci in the perisylvian area, with irregular cortex-white matter junction and a prominent subarachnoid space overlying the cortical malformation (Figure 5A-D). Because the MRI pattern of PMG changes with increasing gestational age, it is important to follow young fetuses at risk and repeat the ultrasound and MRI examinations to confirm the diagnosis. The most common cause of fetal PMG is congenital CMV infection. In these cases, PMG is associated with other signs of brain infection such as: ventriculomegaly, abnormal ventricular lining and adhesions, periventricular pseudocysts, temporal cysts, abnormal echogenicity of the white matter, calcifications, and cerebellar anomalies.

In summary, fetal MCD will probably remain rarely diagnosed in the general population because of the currently recommended routine fetal sonographic screening programs, which are not aimed at late gestational dedicated central nervous system examination. However, as demonstrated in our article, knowledge of the normal fetal cortical developmental landmarks and awareness of the indicative sonographic signs of MCD enable prenatal diagnosis. The prenatal features of MCD are delayed or absent cerebral sulcation; premature abnormal sulci; thin and irregular hemispheric parenchyma; abnormal overdeveloped gyri; wide opening of isolated sulci; nodular bulging into the lateral ventricles; cortical clefts; and intraparenchymal nodules.

### DISCLOSURES

The authors have nothing to disclose.

### REFERENCES

- Leventer RJ, Phelan EM, Coleman LT, Kean MJ, Jackson GD, Harvey AS. Clinical and imaging features of cortical malformations in childhood. *Neurology*. 1999;53:715-22.
- Dobyns WB, Stratton RF, Parke JT, Greenberg F, Nussbaum RL, Ledbetter DH. Miller-Dieker syndrome: lissencephaly and monosomy 17p. *J Pediatr*. 1983;102:552-8.
- Mirzaa GM, Paciorkowski AR. Introduction: brain malformations. *Am J Med Genet C Semin Med Genet*. 2014;166C:117-23.
- Barkovich AJ, Guerrini R, Kuzniecky RI, Jackson GD, Dobyns WB. A developmental and genetic classification for malformations of cortical development: update 2012. *Brain*. 2012;135:1348-1369.
- Andrade CS, Leite Cda C. Malformations of cortical development: current concepts and advanced neuroimaging review. *Arq Neuropsiquiatr*. 2011;69:130-8.
- Malinger G, Lev D, Lerman-Sagie T. Abnormal sulcation as an early sign for migration disorders. *Ultrasound Obstet Gynecol*. 2004;24:704-5.
- Malinger G, Kidron D, Schreiber L, et al. Prenatal diagnosis of malformations of cortical development by dedicated neurosonography. *Ultrasound Obstet Gynecol*. 2007;29:178-91.
- Guibaud L. Contribution of fetal cerebral MRI for diagnosis of structural anomalies. *Prenat Diagn*. 2009;29:420-33.
- Sonigo PC, Rypens FF, Carteret M, et al. MR imaging of fetal cerebral anomalies. *Pediatr Radiol*. 1998;28:212-22.
- Brugger PC, Stühr F, Lindner C, et al. Methods of fetal MR: beyond T2-weighted imaging. *Eur J Radiol*. 2006;57:172-81.

11. Glenn OA, Barkovich J. Magnetic resonance imaging of the fetal brain and spine: an increasingly important tool in prenatal diagnosis: part 2. *Am J Neuroradiol.* 2006;27:1807-14.
12. Limperopoulos C, Clouchoux C. Advancing fetal brain MRI: targets for the future. *Semin Perinatol.* 2009;33:289-98.
13. Glenn OA. Normal development of the fetal brain by MRI. *Semin Perinatol.* 2009;33:208-19.
14. Fong KW, Ghai S, Toi A, et al. Prenatal ultrasound findings of lissencephaly associated with Miller-Dieker syndrome and comparison with pre- and postnatal magnetic resonance imaging. *Ultrasound Obstet Gynecol.* 2004;24:716-23.
15. Chen C-Y, Zimmerman RA, Faro S, et al. MR of the cerebral operculum: topographic identification and measurement of interopercular distances in healthy infants and children. *Am J Neuroradiol.* 1995;16:1677-87.
16. Quarello E, Stirnemann J, Ville Y, et al. Assessment of fetal Sylvian fissure operculization between 22 and 32 weeks: a subjective approach. *Ultrasound Obstet Gynecol.* 2008;32:44-9.
17. Toi A, Chitayat D, Blaser S. Abnormalities of the foetal cerebral cortex. *Prenat Diagn.* 2009;29:355-71.
18. Lerman-Sagie T, Malinge G. Focus on the fetal Sylvian fissure. *Ultrasound Obstet Gynecol.* 2008;32:3-4.
19. Malinge G, Lev D, Lerman-Sagie T. Normal and abnormal fetal brain development during the third trimester as demonstrated by neurosonography. *Eur J Radiol.* 2006;57:226-32.
20. Blondiaux E, Garel C. Fetal cerebral imaging - ultrasound vs. MRI: an update. *Acta Radiol.* 2013;54:1046-54.
21. Guibaud L, Selleret L, Larroche JC, et al. Abnormal Sylvian fissure on prenatal cerebral imaging: significance and correlation with neuropathological and postnatal data. *Ultrasound Obstet Gynecol.* 2008;32:50-60.
22. Guerrini R, Dobyns WB. Malformations of cortical development: clinical features and genetic causes. *Lancet Neurol.* 2014;13:710-726.
23. Abdel Razek AA, Kandell AY, Elsorogy LG, Elmongy A, Basett AA. Disorders of cortical formation: MR imaging features. *AJNR Am J Neuroradiol.* 2009;30:4-11.
24. Saltzman DH, Krauss CM, Goldman JM, et al. Prenatal diagnosis of lissencephaly. *Prenat Diagn.* 1991;11:139-43.
25. Greco P, Resta M, Vimercati A, et al. Antenatal diagnosis of isolated lissencephaly by ultrasound and magnetic resonance imaging. *Ultrasound Obstet Gynecol.* 1991;12:276-9.
26. Crowe C, Jassani M, Dickerman L. The prenatal diagnosis of Warburg syndrome. *Am J Hum Genet.* 1985;37:A214.
27. Rodgers BL, Vanner LV, Pai GS, et al. Walker-Warburg syndrome: report of three affected sibs. *Am J Med Genet.* 1994;49:198-201.
28. Farrell SA, Toi A, Leadman ML, et al. Prenatal diagnosis of retinal detachment in Walker-Warburg syndrome. *Am J Hum Genet.* 1987;28:619-24.
29. Monteagudo A, Alayón A, Mayberry P. Walker-Warburg syndrome: case report and review of the literature. *J Ultrasound Med.* 2001;20:419-26.
30. Gasser B, Lindner V, Dreyfus M, et al. Prenatal diagnosis of Walker-Warburg syndrome in three sibs. *Am J Med Genet.* 1998;76:107-110.
31. Kojima K, Suzuki Y, Seki K, et al. Prenatal diagnosis of lissencephaly (type II) by ultrasound and fast magnetic resonance imaging. *Fetal Diagn Ther.* 2002;17:34-6.
32. Strigini F, Valleriani A, Cecchi M, et al. Prenatal ultrasound and magnetic resonance imaging features in a fetus with Walker-Warburg syndrome. *Ultrasound Obstet Gynecol.* 2009;33:363-5.
33. van Kogelenberg M, Ghedia S, McGillivray G, et al. Periventricular heterotopia in common microdeletion syndromes. *Mol Syndromol.* 2010;1:35-41.
34. Teixeira SR, Blondiaux E, Cassart M, et al. Association of periventricular nodular heterotopia with posterior fossa cyst: a prenatal case series. *Prenat Diagn.* 2015;35:337-41.
35. Mitchell LA, Simon EM, Filly RA, et al. Antenatal diagnosis of subependymal heterotopia. *Am J Neuroradiol.* 2000;21:296-300.
36. Bargallo N, Puerto B, De Juan C, et al. Hereditary subependymal heterotopia associated with mega cisterna magna: antenatal diagnosis with magnetic resonance imaging. *Ultrasound Obstet Gynecol.* 2002;20:86-9.
37. Stutterd CA, Leventer RJ. Polymicrogyria: a common and heterogeneous malformation of cortical development. *Am J Med Genet C Semin Med Genet.* 2014;166C:227-39.
38. Barkovich AJ. Current concepts of polymicrogyria. *Neuroradiology.* 2010;52:479-87.
39. Leventer RJ, Jansen A, Pilz DT, et al. Clinical and imaging heterogeneity of polymicrogyria: a study of 328 patients. *Brain.* 2010;133:1415-27.
40. Fogliarini C, Chaumoitre K, Chapon F, et al. Assessment of cortical maturation with prenatal MRI. Part I: normal cortical maturation. *Eur Radiol.* 2005;15:1671-85.